Molecular Crystals and Liquid Crystals

Publication details, including instructions for authors and subscription information:
http://www.tandfonline.com/loi/gmcl20

# Efficiency Stabilized Deep Blue Organic Light-Emitting Devices with a DPVBi/CBP Step Emitting Layer Operating at Low Voltages

H. S. Bang [a], D. U. Lee [a], T. W. Kim [a], J. H. Kim [b], J. H. Seo [c] & Y. K. Kim [c]

[a] Research Institute of Information Display, Division of Electronics and Computer Engineering, Hanyang University, Seoul, Korea

[b] Department of Electronics Engineering, Hong-ik University, Seoul, Korea

[c] Department of Information Display Engineering & Center for Organic Materials & Information Display (COMID), Hong-ik University, Seoul, Korea

Version of record first published: 22 Sep 2010

To cite this article: H. S. Bang, D. U. Lee, T. W. Kim, J. H. Kim, J. H. Seo & Y. K. Kim (2007): Efficiency Stabilized Deep Blue Organic Light-Emitting Devices with a DPVBi/CBP Step Emitting Layer Operating at Low Voltages, Molecular Crystals and Liquid Crystals, 470:1, 259-267

To link to this article: http://dx.doi.org/10.1080/15421400701495948

*Mol. Cryst. Liq. Cryst.*, Vol. 470, pp. 259–267, 2007

ISSN: 1542-1406 print/1563-5287 online
DOI: 10.1080/15421400701495948



# Efficiency Stabilized Deep Blue Organic Light-Emitting Devices with a DPVBi/CBP Step Emitting Layer Operating at Low Voltages

**H. S. Bang**
**D. U. Lee**
**T. W. Kim**
Research Institute of Information Display, Division of Electronics and Computer Engineering, Hanyang University, Seoul, Korea

**J. H. Kim**
Department of Electronics Engineering, Hong-ik University, Seoul, Korea

**J. H. Seo**
**Y. K. Kim**
Department of Information Display Engineering & Center for Organic Materials & Information Display (COMID), Hong-ik University, Seoul, Korea

*The electrical and the optical properties of deep blue organic light-emitting devices (OLED) utilizing a step emitting layer (SEL) consisting of 4,4′-Bis(2,2′-diphenylethen-1-yl)biphenyl (DPVBi) and 4,4′-Bis(carbazol-9-yl)biphenyl (CBP) were investigated. The turn-on voltage of the OLEDs with a SEL was smaller than those of the OLEDs with a CBP or a DPVBi emitting layer. While the efficiency of the OLEDs with a SEL was very stable, regardless of variations in the applied voltage, that of the OLEDs with a CBP or a DPVBi emitting layer varied with the applied voltage. The dominant peak in the electroluminescence spectrum for the OLEDs with a SEL appeared at 455 nm. The Commission Internationale de l'Eclairage chromaticity (CIE) coordinates of the OLEDs with a SEL at 11 V were (0.160, 0.168), which is similar to the CIE coordinates of the CBP layer.*

This work was supported by the Korea Research Foundation Grant funded by the Korean Government (MOEHRD, Basic Research Promotion Fund) (KRF-2006-005-J04102).

Address correspondence to T. W. Kim, Research Institute of Information Display, Division of Electronics and Computer Engineering, Hanyang University, 17 Haengdang-dong, Seongdong-gu, Seoul 133-791, Korea. E-mail: twk@hanyang.ac.kr

**Keywords:** deep blue organic light-emitting device; electrical properties; optical properties; step emitting layer

**PACS Numbers:** 78. 60. Fi, 78. 66. Qn, and 73. 20. At



## I. INTRODUCTION

Recently, organic light-emitting diodes (OLEDs) have been particularly attractive because of the interest in promising applications in promising next-generation full-color flat-panel displays because they have the unique advantages of low driving voltage, low power consumption, high color gamut, high contrast, and fast response [1–4]. The potential applications of novel high-efficiency blue OLEDs have driven extensive efforts to fabricate OLEDs with unique structures [5]. However, the blue OLEDs for practical utilization in full-color flat-panel displays still have inherent several problems of low efficiency, poor color purity, and short lifetime in comparison with red or green OLEDs [6]. This has driven extensive efforts to overcome these inherent problems, resulting in fabrication of the blue OLEDs with high efficiency, good color stabilization, and long lifetime. OLEDs with various structures were suggested for enhancing their efficiency and the color stabilization [7–12]. Even though some works on enhancing the efficiency and color stability in blue OLEDs utilizing a doped layer or a hole-blocking layer (HBL) have been performed to enhance the balance of holes and electrons in an emitting layer (EML) [13–18], the problems of the low efficiency, the poor-color purity, and the short lifetime in the blue OLEDs have been remained. Therefore, systematic studies on blue OLEDs utilizing a step emitting layer (SEL) without exciton quenching effects are necessary for achieving high efficiency and good color stability of these devices.

This article reports the electrical and the optical properties of blue OLEDs with a SEL deposited by using organic molecular-beam deposition (OMBD). Current density-voltage (J-V) measurements were performed to investigate the electrical properties of the OLEDs with a SEL consisting of 4,4′-Bis(2,2-diphenyl-ethen-1-yl)biphenyl (DPVBi) and 4,4′-Bis(carbazol-9-yl)biphenyl (CBP), with a DPVBi single EML, or with a CBP single EML. Luminance-voltage, efficiency-current density, and electroluminescence (EL) measurements were carried out to investigate the efficiency and the color stabilization of OLEDs with three kinds of structures. The Commission Internationale de l'Eclairage (CIE) chromaticity coordinates corresponding to

the emission colors for OLEDs with three kinds of structures were determined to investigate the blue color stabilization. The electrical and the optical properties of the OLEDs with a SEL were compared with those of OLEDs with a DPVBi layer or a CBP layer.

## II. EXPERIMENTAL DETAILS

The sheet resistivity and the thickness of the indium-tin-oxide (ITO) thin films coated on glass substrates used in this study were 15 Ω/ sq. and 100 nm, respectively. The ITO substrates were cleaned using ultrasonications in acetone, methanol, and distilled water at 60°C for 15 min and were rinsed in de-ionized water thoroughly. The chemically cleaned ITO substrates were kept for 48 h in isopropyl alcohol. After the chemically cleaned ITO substrates had been dried by using $N_2$ gas with a purity of 99.9999%, the surfaces of the ITO substrates were treated with an oxygen plasma for 2 min at an $O_2$ pressure of approximately $2 \times 10^{-2}$ Torr. The three kinds of samples used in this study were deposited on ITO thin films coated on glass substrates by using OMBD with tungsten effusion cells and shutters in a growth chamber at a pressure of $5 \times 10^{-6}$ Torr and consisted of the following structures from the top: an aluminum (Al) (100 nm) cathode electrode, a lithium quinolate (Liq) (2 nm) electron injection layer (EIL), a tris(8-hydroxyquinolate) aluminum ($Alq_3$) (25 nm) electron transport layer (ETL), a 2,9-dimethyl-4,7-diphenyl-1,10-phenanthroline (BCP) (5 nm) hole blocking layer HBL, various kinds of the EMLs, an N,N′-Bis(-naphthalene-1-yl)-N,N′-bis(phenyl)-benzidine (NPB) (50 nm) HTL, an ITO anode electrode, and a glass substrate. The EMLs consisted of a 4,4′-Bis(2,2′-diphenyl-ethen-1-yl)biphenyl (DPVBi) (30 nm), a 4,4′-Bis(carbazol-9-yl)biphenyl (CBP) (30 nm), or a DPVBi (15 nm)/CBP (15 nm) SEL. After organic and metal depositions, the OLED devices were encapsulated in a glove box with $O_2$ and $H_2O$ concentrations below 1 ppm. A desiccant material consisting of a barium-oxide powder was used to absorb the residual moisture and oxygen in the encapsulated device. The Liq layer, acting as an EIL, leads to a lower turn-on voltage and a higher power efficiency [19]. The deposition rates of the organic layers and the metal layers were approximately 0.1 and 0.15 nm/s, respectively, and the deposition rates were controlled by using a quartz crystal monitor. The emitting area in the pixel was 3 $\times$ 3 $mm^2$. The J-V characteristics of the OLEDs were measured on a programmable electrometer with built-in current and voltage measurement units (model SMU-236, Keithely). The brightness was measured by using a brightness meter, chroma meter CS-100A (Minolta).

## III. RESULTS AND DISCUSSION

The schematic energy diagrams of the fabricated OLEDs of devices (a) I, (b) II, and (c) III are shown in Figure 1. The conventional blue OLEDs with a DPVBi or a CBP EML are shown in Figures 1(a) and 1(b), respectively, and the unique blue OLED with a DPVBi/CBP SEL is shown in Figure 1(c). The highest occupied molecular orbital (HOMO) and the lowest unoccupied molecular orbital (LUMO) levels of the NPB are −5.5 and −2.5 eV, as obtained by using cyclic voltammerty, respectively [20], and the HOMO and the LUMO levels of the CBP layer are −6.3 and −3.2 eV, respectively [21]. The HOMO and the LUMO levels of the DPVBi layer are −5.9 and −2.8 eV, respectively [22], and the corresponding levels of the BCP layer are −6.7 and −3.2 eV, respectively [23]. While the electrons are accumulated in the DPVBi/CBP step layer due to the existence of the DPVBi EML in device III, the holes are accumulated in the DPVBi/CBP step layer due to the existence of the CBP EML in device III, resulting in an

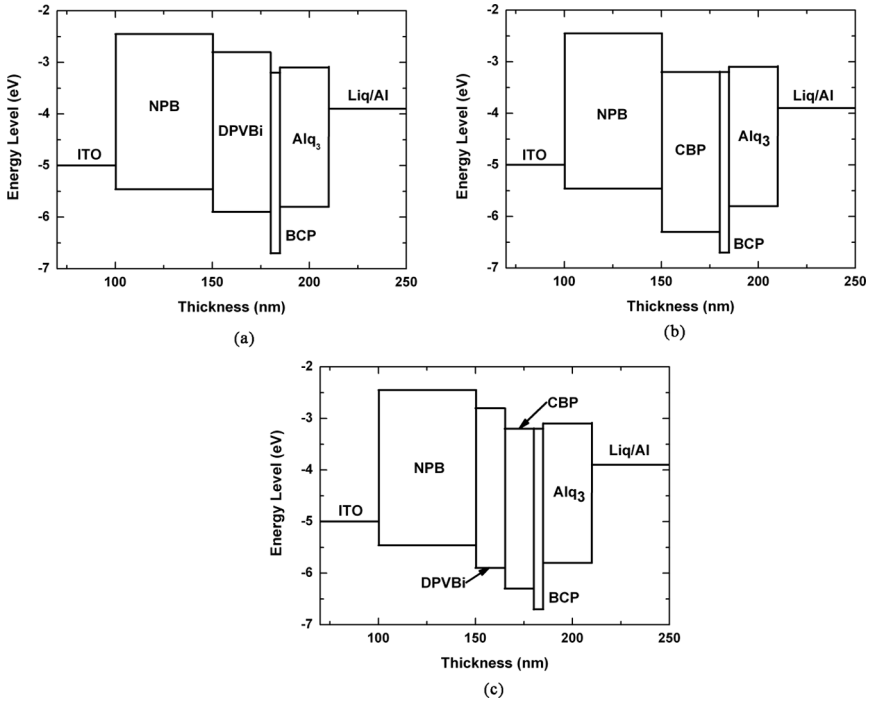


**FIGURE 1** Schematic energy band diagrams for the OLEDs of devices (a) I, (b) II, and (c) III.

increase in the number of electrons and holes at DPVBi/CBP hetero-interfaces.

Figure 2 shows (a) the log scale current densities as functions of the applied voltage (log J-log V), (b) the luminance as functions of the applied voltage, and (c) the efficiencies as functions of the current density for the OLEDs with three structures. Filled rectangles, circles, and triangles represent the OLEDs of devices I, II, and III, respectively. The log J-log V characteristics show that the turn-on voltage of the OLED with a SEL was smaller than those of the OLEDs with a DPVBi or a CBP EML. The turn on voltage of the OLED with a SEL decreased as much as 0.5 V in comparison with those of the OLEDs with a DPVBi or a CBP EML, as determined from the log J-log V curves. The decrease in the turn-on voltage of the OLED with a SEL was attributed to the easy movement of the electrons and holes

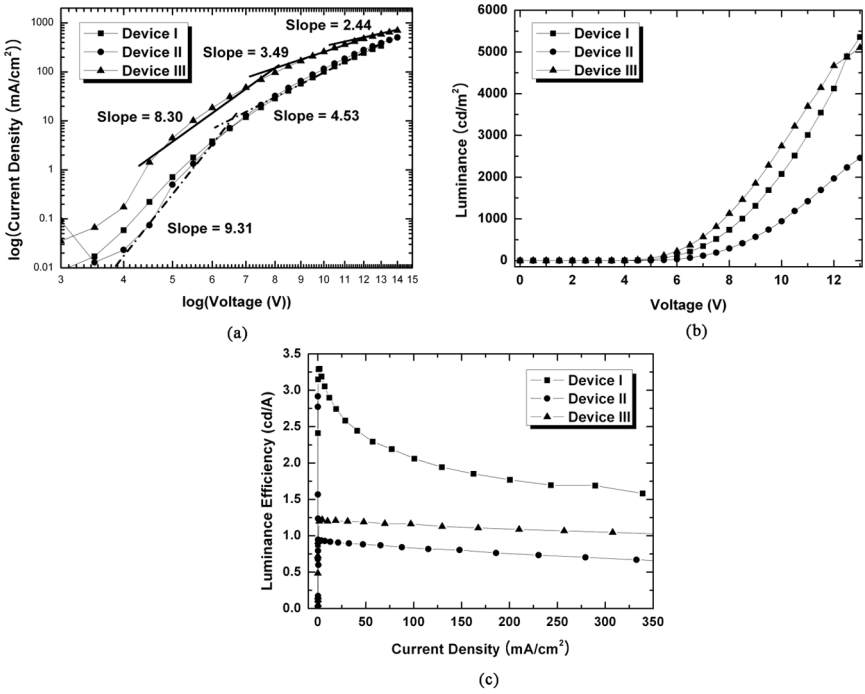


**FIGURE 2** (a) Log scale current densities as functions of the applied voltage, (b) luminance as functions of the applied voltage, and (c) luminance efficiencies as functions of the current density for OLEDs with three structures. Filled rectangles, circles, and triangles represent the OLEDs of devices I, II, and III, respectively.

toward the DPVBi/CBP heterointerfaces, resulting in the efficient formation of the exciton recombination. While the electrons are accumulated in the DPVBi/CBP step layer due to the existence of the DPVBi EML in device III, as shown in the LUMO level of the Figure 1(c), the holes are accumulated in the DPVBi/CBP step layer due to the existence of the CBP EML in device III, as shown in the HOMO level of the Figure 1(c), resulting in an increase in the number of electrons and holes at DPVBi/CBP heterointerfaces.

While the log J-log V characteristics of device III show trap charge limit current (TCLC) region and space charge limit current (SCLC) region, those of devices I and II show only the TCLC region. If the equation for the relationship between current (J) and voltage (V) at the TCLC and the SCLC regions $J = \frac{9}{8}\varepsilon_0\varepsilon_r\mu_0\frac{V^n}{d^3}$ is used [24], where, $\varepsilon_0$ is the dielectric constant of vacuum, $\varepsilon_r$ is the dielectric constant of organic material, $\mu_0$ is the mobility of the device, V is the applied voltage, $d$ is the device thickness, $n$ can be fitted. The $n$ values at SCLC and TCLC regions, as determined from the log J-log V curves, are shown in Figure 2(a). Because the high voltage region of device III corresponds to the SCLC region the electrons and the holes are highly accumulated at the DPVBi/CBP heterointerfaces, resulting in exciton recombination. The luminance as functions of the applied voltage depict that the turn-on voltage of device III is smaller than those of devices I and II, and that the luminescence of device III is higher than those of devices I and II, as shown in Figure 2(b). Even though the turn-on voltage of device III is low, the maximum luminance of device III is almost same as that of device I and is as twice as that of device II, indicative of high luminance and low turn-on voltage of device III.

The luminance efficiencies as functions of the current density for devices I, II, and III are shown in Figure 2(c). Even though the efficiency of device I is highest among three devices, the efficiency significantly decreases with increasing current density. The dramatic decrease in the luminance efficiency of device I is related to the creation of the joule heating due to the nonradiative recombination process resulting from the phonon scattering, resulting in a significant decrease of the lifetime of device I. The decrease rates of the luminance efficiencies in devices II and III are much smaller than that in device I. In particular, the luminance efficiency of device III is almost constant, regardless of the variation of the current density, indicative of the lowest existence of the exciton quenching effect without annihilation effect.

Figure 3 shows the EL spectra at 11 V for devices I, II, and III. The dominant peaks at 463, 450, and 455 nm for EL spectra of devices I, II, and III appears, respectively, and the corresponding full width at half maximum (FWHM) of the EL spectra are 68, 67, and 68 nm,

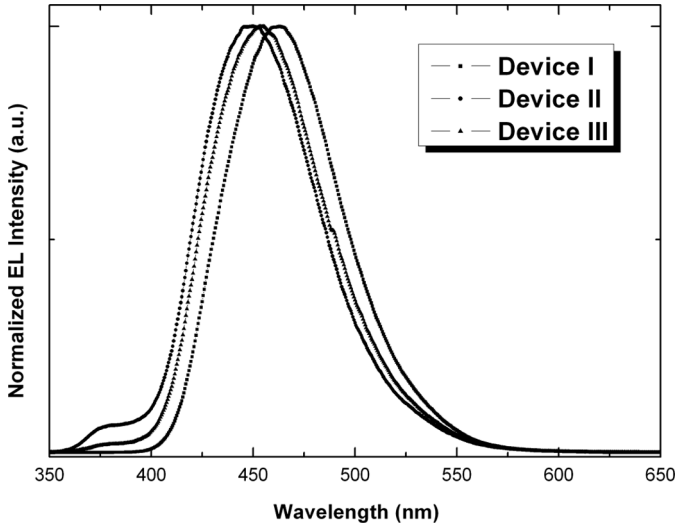


**FIGURE 3** Electroluminescence spectra at 11 V for OLEDs with three structures. Filled rectangles, circles, and triangles represent the OLEDs of devices I, II, and III, respectively.

respectively. The dominant peak for the EL spectrum of device III is located between the luminescence peak of the DPVBi EML and the CBP EML, which shifts to higher energy in comparison with that of device I and shifts to lower energy in comparison with that of device II. The luminescence peaks related to the DPVBi and the CBP layer appears at device III, resulting in the extension of the emitting layer, and a shoulder at 380 nm corresponding to the luminescence peak of the BCP layer appears at devices II and III.

Figure 4 shows CIE coordinates at 11 V for OLEDs of devices I, II, and III. The CIE coordinates of devices I, II, and III are (0.160, 0.203), (0.163, 0.164), and (0.160, 0.168), respectively. The CIE chromaticity coordinates of device II and III is much closer to the blue coordinates of the national television system committee standard (0.140, 0.08) than that of device I. Since the blue emission spectrum corresponding to the blue color for OLEDs with a CBP layer is deeper than that with a DPVBi layer, the emission region of the OLEDs with a SEL consisting of a DPVBi layer and a CBP layer is covered over the DPVBi layer and the CBP layer. Furthermore, because the intensity of the additional spectrum emitted form the DPVBi layer in the SEL between the DPVBi layer and the CBP layer is lower, decreased the color stability of device III with a SEL becomes enhanced.

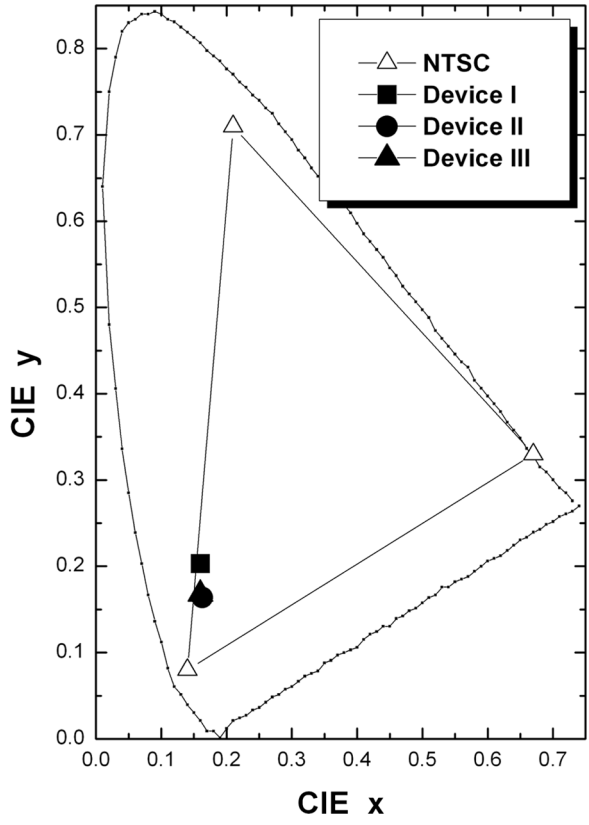


**FIGURE 4** Commission Internationale de l'Eclairage (CIE) coordinates at 11 V for the OLEDs with three structures. Filled rectangles, circles, and triangles represent the OLEDs of devices I, II, and III, respectively. Empty triangles indicate the CIE coordinates of the national television system committee standard.

## IV. SUMMARY AND CONCLUSIONS

The electrical and the optical properties of OLEDs with a DPVBi EML, a CBP EML, or a DPVBi/CBP SEL were investigated. The turn-on voltage of the OLEDs with a SEL was smaller than those of the OLEDs with a CBP or a DPVBi emitting layer. While the efficiency of the OLEDs with a SEL was stable, regardless of the variation of the applied voltage, that of the OLEDs with a DPVBi layer or a CBP layer varied with applied voltage. The EL spectrum for the OLEDs with a SEL showed a dominant EL peak corresponding to the

deep-blue region. The CIE coordinates with a SEL at 11 V were (0.160, 0.168), indicative of a deep, stabilized blue color. These results indicate that efficiency-stabilized blue OLEDs can be fabricated using a DPVBi/CBP SEL.

## REFERENCES


[1] Tang, C. W., Van Slyke, S. A., & Chen, C. H. (1989). *J. Appl. Phys.*, *65*, 3610.
[2] Adachi, C., Tsutsui, T., & Saito, S. (1989). *Appl. Phys. Lett.*, *55*, 1489.
[3] Rothberg, L. J. & Lovinger, A. J. (1996). *J. Mater. Res.*, *11*, 3174.
[4] Hung, L. S. & Chen, C. H. (2002). *Mater. Sci. Eng. R*, *38*, 143.
[5] Holmes, R. J., Forrest, S. R., Sajoto, T., Tamayo, A., Djurovich, P. I., Thompson, M. E., Brooks, J., Tung, Y. J., D'Andrade, B. W., Weaver, M. S., Kwong, R. C., & Brown, J. J. (2005). *Appl. Phys. Lett.*, *87*, 243507.
[6] Li, G. & Shinar, J. (2003). *Appl. Phys. Lett.*, *83*, 5359.
[7] Cheng, G., Zhang, Y., Ziao, Y., Liu, S., Xie, Z., Xia, H., Hanif, M., & Ma, Y. (2005). *Appl. Phys. Lett.*, *87*, 013506.
[8] Hsu, S. F., Lee, C. C., Hwang, S. W., Chen, H. H., Chen, C. H., & Hu, A. T. (2005). *Thin Solid Films.*, *478*, 271.
[9] Wang, Y. M., Teng, F., Zhou, Q. C., & Wang, Y. S. (2006). *Applied Surface Science*, *252*, 2355.
[10] Shaheen, S. E., Jabbour, G. E., Morrell, M. M., Kawabe, Y., Kippelen, B., peyghambarian, N., Nabor, M. F., Schlaf, R., Mash, E. A., & Armstrong, N. R. (1998). *Appl. Phys. Lett.*, *84*, 2324.
[11] Adamovich, V. I., Cordero, S. R., Djurovich, P. I., Tamayo, A., Thompson, M. E., D'Andrade, B. W., & Forrest, S. R. (2003). *Organic Electronics.*, *4*, 77.
[12] Trattnig, G., Pogantsch, A., Langer, G., Kern, W., & Zojer, E. (2002). *Appl. Phys. Lett.*, *81*, 4269.
[13] Liu, S. W., Huang, C. A., Yang, J. H., Chen, C. C., & Chang, Y. (2004). *Thin Solid Films.*, *453–454*, 312.
[14] Lu, H. T., Tsou, C. C., & Yokoyama, M. (2005). *J. Crystal Growth.*, *277*, 388.
[15] Zou, L., Savvate'ev, V., Booher, J., Kim, C. H., & Shinar, J. (2001). *Appl. Phys. Lett.*, *79*, 2282.
[16] Gebeyehu, D., Walzer, K., He, G., Pfeiffer, M., Leo, K., Brandt, J., Gerhard, A., Stößel, P., & Vestweber, H. (2005). *Synth. Met.*, *148*, 205.
[17] Im, W. B., Hwang, H. K., Lee, J. G., Han, K. J., & Kim, Y. K. (2001). *Appl. Phys. Lett.*, *79*, 1387.
[18] Chen, B., Zhang, X. H., Lin, X. Q., Kwong, H. L., Wong, N. B., Lee, C. S., Gambling, W. A., & Lee, S. T. (2001). *Synth. Met.*, *118*, 193.
[19] Wu, C. C., Lin, Y. T., Chiang, H. H., Cho, T. Y., Chen, C. W., Wong, K. T., Liao, Y. L., Lee, G. H., & Peng, S. M. (2002). *Appl. Phys. Lett.*, *81*, 577.
[20] Hamada, Y., Kanno, H., Tsujioka, T., Takahashi, H., & Usuki, T. (1999). *Appl. Phys. Lett.*, *75*, 1682.
[21] Adachi, C., Baldo, M. A., & Forrest, S. R. (2000). *J. Appl. Phys.*, *87*, 8049.
[22] Hosokawa, C., Higashi, H., Nakamura, H., & Kusumoto, T. (1995). *Appl. Phys. Lett.*, *67*, 3853.
[23] Tsou, C. C., Lu, H. T., & Yokoyama, M. (2005). *J. Crystal Growth*, *280*, 201.
[24] Ogawa, T., Cho, D. C., Kaneko, K., Mori, T., & Mizutani, T. (2003). *Thin Solid Films*, *438*, 171.